# Design, synthesis and cholinesterase inhibitory activity of new dispiro pyrrolidine derivatives

Nadia Mohamed Yusoff, Hasnah Osman, Valentia Katemba, Muhammad Solehin Abd Ghani, Unang Supratman, Mohammad Tasyriq Che Omar, Vikneswaran Murugaiyah, Xiang Ren, Yvan Six, Mohamad Nurul Azmi

**Design, Synthesis and Cholinesterase Inhibitory Activity of New Dispiro Pyrrolidine Derivatives**

Nadia Mohamed Yusoff [a], Hasnah Osman [a], Valentia Katemba [b], Muhammad Solehin Abd Ghani [a], Unang Supratman [c], Mohammad Tasyriq Che Omar [d], Vikneswaran Murugaiyah [e,f], Xiang Ren [g], Yvan Six [g,*] and Mohamad Nurul Azmi [a,*]

[a] *School of Chemical Sciences, Universiti Sains Malaysia, 11800 Minden, Penang, Malaysia*

[b] *Institute of Pharmaceutical Science, King's College London, Franklin Wilkins Building, Stamford Street, London, SE1 9NH*

[c] *Department of Chemistry, Faculty of Science and Mathematics, Universitas Padjadjaran, Jatinangor, 45363 West Java, Indonesia*

[d] *Biological Section, School of Distance Education, Universiti Sains Malaysia, 11800 Penang, Malaysia*

[e] *Centre for Drug Research, Universiti Sains Malaysia, 11800 Minden, Penang, Malaysia.*

[f] *School of Pharmaceutical Sciences, Universiti Sains Malaysia, 11800 Minden, Penang, Malaysia*

[g] *Laboratoire de Synthèse Organique (LSO), UMR 7652 CNRS/ENSTA/École Polytechnique, Institut Polytechnique de Paris, 91128 Palaiseau Cedex, France*

[*]Corresponding author: mnazmi@usm.my / yvan.six@polytechnique.edu

**Abstract**

A series of new dispiro pyrrolidines were regioselectively synthesised via [3+2]-cycloaddition reactions of 3,5-bis(arylidene)-1-phenylethyl-4-piperidones with azomethine ylides generated in situ from *N*-methylglycine and appropriate isatin derivatives. The structures of the synthesised compounds were characterised by NMR, FT-IR and MS. These compounds were assayed *in vitro* for their inhibitory activity against acetylcholinesterase (AChE) and butyrylcholinesterase (BChE), using Ellman's assay. The results demonstrate better inhibitory activity against butyrylcholinesterase as compared to acetylcholinesterase. Compound **7b** exhibits potential as a new BChE inhibitor, with an $IC_{50}$ of 12.78 ± 1.52 μM. A kinetic study suggests **7b** as a mixed-mode inhibitor, where the active molecule can bind to the active or allosteric sites of the enzyme. An *in silico* study was performed using AutoDock Vina to identify the binding energy and conformation of **7b** with the crystal structure of BChE complexed with Thioflavin T (PDB ID: 6ESY) and the crystal structure of human AChE complexed with dihydrotanshinone 1 (PDB ID: 4M0E). The results indicate better binding properties of **7b** compared with the standard inhibitor Thioflavin T, with calculated binding energies of –13.9 and –9.7 kcal $mol^{-1}$ for BChE and AChE, respectively.

**Keywords:** Dispiro pyrrolidine; Dispiro heterocycle; 1,3-Dipolar cycloaddition; Cholinesterase; Molecular docking

## 1. Introduction

Spiro compounds represent an important class of naturally occurring compounds found in plants and animals [1]. A number of studies have shown that various 2-indolone compounds (oxindoles) having a spiro system are of particular interest and can exhibit promising and diversified biological activities [2-4], such as anticancer [5-7], anti-Alzheimer [8-10],

antidiabetic [11], antimicrobial [12-14], antituberculosis [12-15], antiviral [16], local anesthetic [17], antileukemic and anticonvulsant [18]. The widely known biological potency of spiro compounds and oxindoles has led researchers to investigate and synthesise new spiro heterocyclic compounds comprising oxindole and pyrrolidine moieties.

Alzheimer's disease (AD) is a multifarious neurodegenerative disorder. It is the most prevalent form of dementia that may contribute 60-70% of cases. According to the World Health Organisation (WHO), the symptoms of Alzheimer's patients are manifested by progressive deterioration of cognitive function, intellectual decline, memory loss and personality change [19]. Currently, around 55 million people suffer from AD worldwide, and almost 10 million new cases are reported each year. The number of people living with dementia is estimated to reach 78 million in 2030 and 139 million by 2050 [19]. Studies have shown that women are more frequently affected by AD, with 16% prevalence at the age of 71 and above, compared to 11% of men. People with higher education years are reported to be at lower risk [20].

Acetylcholine (ACh) is an important neurotrasmitter that helps transfer nerve messages in the human central nervous system. A low concentration of Ach arising from neurodegeneration and reduced availability of choline acetyltransferase prompts the development of the symptoms of AD [21]. Cholinesterases are the enzymes responsible for breaking down Ach. The brain contains two types of cholinesterases: acetylcholinesterase (AChE) and butyrylcholinesterase (BChE). Both of them are hydrolytic enzymes that react with ACh and terminate its actions at the synaptic cleft by cleaving the neurotransmitter to choline and acetate ion [22-23]. Therefore, one of the strategies for the treatment of AD is to find an inhibitor that can inhibit AChE and BChE, thus prolonging the availability of Ach at the synaptic cleft. Examples of such cholinesterase inhibitors that are available on the market to treat AD patients include rivastigmine, donepezil and galantamine.

In this context and based on our previous work on this series [8-10], we are now reporting the synthesis of new dispiro pyrrolidine derivatives, as well as their cholinesterase inhibitory properties, evaluated against AChE and BChE. These experimental data are completed by molecular modelling studies that help understand the interaction of the most active inhibitor with the appropriate target active site of the cholinesterase enzymes.

## 2. Results and Discussions

### 2.1. Synthesis of dispiro pyrrolidine compounds

The target dispiro pyrrolidine compounds **7a-h** were synthesised by 1,3-dipolar cycloaddition reactions of azomethine ylides, generated *in situ* by decarboxylative condensation of sarcosine **6** with isatin derivatives **5a-d**, in the presence of 3,5-bis(arylidene)-1-phenethyl-4-piperidinone **3** or **4** as appropriate dipolarophiles (Scheme 1) [5-7,24, 33-34].

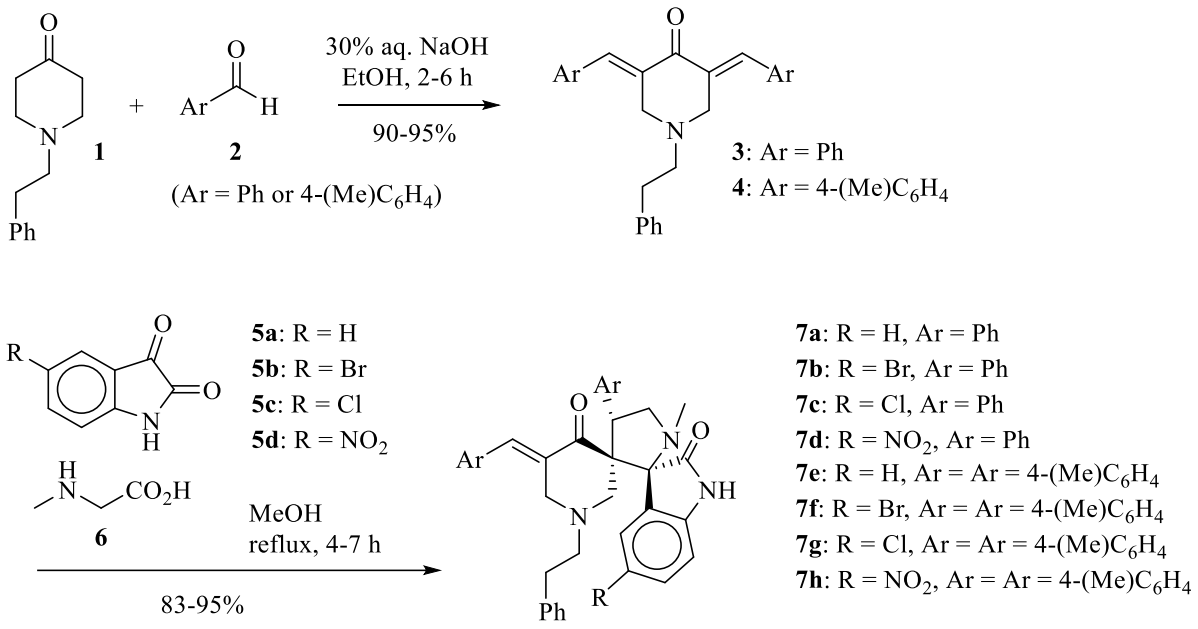


**Scheme 1** Synthesis of spiro pyrrolidine derivatives **7a-h**.

The cycloadducts were obtained in good to excellent yields (83-95%). Their structures were confirmed by spectroscopic techniques including 1D- and 2D-NMR, FT-IR and HRMS (see supplementary data). Remarkably, all these products were obtained as single diastereoisomers. The relative configurations of their chiral centres were established by comparison of key $^{13}C$ NMR chemical shifts with those of closely related compounds, the structures of which have been unambiguously determined by X-ray crystallography in previous work [5-7,32-33]. For instance, the chemical shifts of the carbon atoms located around the chiral centres of **7a** were all found to be different from those of the known molecule **8** by no more than 1.1 ppm (average deviation 0.5 ppm; Table 1) [32]. Furthermore, in the comparison of **7g** and the analogous compound **9**, [5] the maximal difference was found to be 0.2 ppm (Table 2). In addition, **8** and **9** were synthesised using the same route as **7a** and **7g**. Therefore, the relative configurations of the latter can be very safely assigned as shown in Scheme 1. The same $^{13}C$ NMR shift comparative process strongly supports identical relative configurations in **7a**, **7c** and **7e**. From there, it is reasonable to assume that all adducts **7a-h** have the same relative configurations.

**Table 1** Comparison of selected $^{13}C$ NMR chemical shifts of product **7a** with literature compound **8** [32].

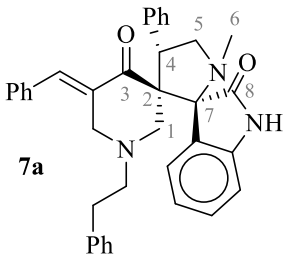


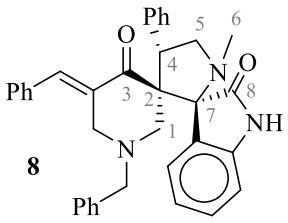


| | Compound **7a** $\delta$ ($CDCl_3$) (ppm) | Compound **8** $\delta$ ($CDCl_3$) (ppm)[32] |
|---|---|---|
| C1 | 57.0 | 57.0 or 57.1 |
| C2 | 66.1 | 65.7 |
| C3 | 198.9 | 199.1 |
| C4 | 45.6 | 46.3 |
| C5 | 56.2 | 57.0 or 57.1 |
| C6 | 34.6 | 34.7 |
| C7 | 75.0 | 76.1 |
| C8 | 176.7 | 177.4 |

**Table 2** Comparison of selected $^{13}C$ NMR chemical shifts of product **7g** with literature compound **9** [5].

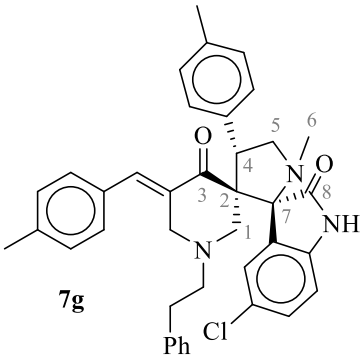


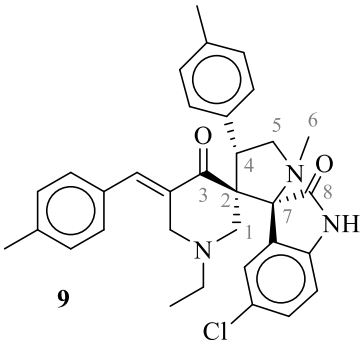


| | Compound **7g** $\delta$ (DMSO-$d_6$) (ppm) | Compound **9** $\delta$ (DMSO-$d_6$) (ppm)[5] |
|---|---|---|
| C1 | 56.8 or 56.9 | 56.8 or 56.9 |
| C2 | 65.4 | 65.2 |
| C3 | 198.6 | 198.7 |
| C4 | 45.1 | 45.0 |
| C5 | 56.8 or 56.9 | 56.8 or 56.9 |
| C6 | 34.6 | 34.7 |
| C7 | 75.7 | 75.8 |
| C8 | 176.7 | 176.7 |

The proposed reaction mechanism for the formation of the dispiro pyrrolidine cycloadducts is shown in Scheme 2. First, a condensation reaction takes place between the secondary amine function of sarcosine **6** and the carbonyl group of isatin **5a-d** located at C-3. The iminium intermediate thus generated, which is thought to be in equilibrium with a cyclic hemiaminal ester, eventually loses carbon dioxide, irreversibly, to produce the key azomethine ylide species **11a-d**. Regio- and stereo-selective [3+2] cycloaddition with **3** or **4** then operates to produce the dispiro pyrrolidines **7a-h**, respectively [31]. Since the various elementary steps of this mechanism involve polar or charged species, the choice of methanol, a polar protic solvent, ensures a comparatively short reaction time, by stabilisation of the transition states involved [31,35]. The exclusive formation of *mono* adducts is most likely due to the steric hindrance of the remaining C=C exocyclic double bond, which prevents further reaction with the 1,3-dipole [36].

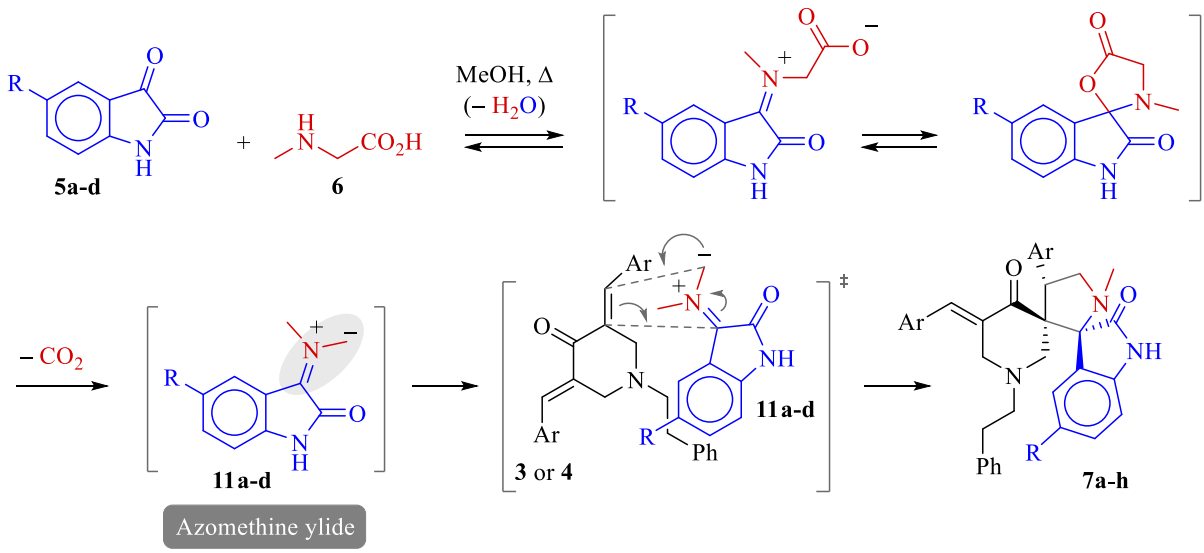


**Scheme 2** Mechanism for the formation of the cycloadducts **7a-h**

## 2.2. Cholinesterase inhibitory activity of the target molecules

The new series of dispiro pyrrolidines **7a-h** were evaluated *in vitro* for their potential as inhibitors of cholinesterases (AChE or BChE), with physostigmine as a positive control. Hydrolysis of the respective substrate used in the Ellman assay by the enzymes (acetylthiocholine by AChE and butyrylthiocholine by BChE) releases yellow-coloured 5-thio-2-nitrobenzoate, with an absorption maximum at 412 nm. Recording of the decrease in absorbance thus allows measuring the inhibition of the enzyme activities, as a result of the effect of the molecules being evaluated. The inhibitions of AChE and BChE at 10 µM for series **7a-h** are summarised in Table 3. It is worthy of note that as a potent cholinesterase inhibitor, the reference drug physostigmine was used at a lower concentration in the bioassay, 0.20 µM, to avoid complete inhibition of the enzymatic activities. In summary, the compounds showed weak to moderate inhibitory activity against both cholinesterases.

Most of the compounds displayed higher inhibitory activities against BChE than against AChE. Structural features of AChE and BChE, especially at the active site gorge confer differences in their substrate specificity [37]. AChE is highly selective to Ach, while BChE can metabolize various molecules apart from Ach. Although both enzymes share 65% amino-acid sequence homology, most of the aromatic amino acid residues at the BChE active site are replaced by amino acid residues with hydrophobic aliphatic side chains such as valine (Val) and leucine (Leu) instead of phenylaniline (Phe), tryptophan (Typ) and tyrosine (Tyr) in AChE, making BChE able to incorporate bulkier substrate and inhibitors in its active site [10]. This could provide an explanation for the higher inhibition values observed toward BChE, compared to AChE.

Out of eight new dispiro pyrrolidines, compound **7b** was the only one that showed more than 50% inhibition at 10 µM. The presence of a bromo substituent at the oxindole moiety appears to have a positive impact on the inhibition of BChE. This is to be compared to a

previous study, where the presence of a chlorine atom at the aromatic ring of the oxindole had a positive effect on BChE inhibition [27]. However, other halogen atoms (bromine or fluorine) were not evaluated in that particular study. It is interesting to note that despite being the strongest inhibitor of BChE, compound **7b** exhibited the lowest level of inhibition on AChE among the derivatives, suggesting that **7b** could be a BChE-selective inhibitor. Consequently, $IC_{50}$ determination against BChE was undertaken for compound **7b** only, giving a value of 12.78 ± 1.52 μM. This activity can be categorized as moderate, compared to the standard drug physostigmine, which has a reported $IC_{50}$ value of 0.16 μM on BChE [27].

**Table 3** Cholinesterase inhibitory activity of spiro pyrrolidines **7a-h**.

| Entry | Compound | Ar | R | % Inhibition at 10 μM | |
|---|---|---|---|---|---|
| | | | | AChE | BChE |
| **1** | **7a** | Ph | H | 21.87 ± 4.91 | 37.66 ± 4.33 |
| **2** | **7b** | Ph | Br | 13.49 ± 3.47 | 63.25 ± 7.25 |
| **3** | **7c** | Ph | Cl | 43.50 ± 5.70 | 47.99 ± 3.13 |
| **4** | **7d** | Ph | $NO_2$ | 39.49 ± 8.14 | 43.65 ± 4.58 |
| **5** | **7e** | 4-(Me)$C_6H_4$ | H | 39.54 ± 4.84 | 41.64 ± 4.53 |
| **6** | **7f** | 4-(Me)$C_6H_4$ | Br | 29.75 ± 4.28 | 44.78 ± 4.49 |
| **7** | **7g** | 4-(Me)$C_6H_4$ | Cl | 37.17 ± 5.13 | 30.68 ± 3.94 |
| **8** | **7h** | 4-(Me)$C_6H_4$ | $NO_2$ | 28.60 ± 9.14 | 48.27 ± 5.79 |
| **Reference standard** | Physostigmine (tested at 0.2 μM) | | | 70.13 ± 2.37 | 47.62 ± 2.23 |

All data are presented as mean ± standard error, SE (n=3).

### 3.3. Kinetic study of BChE inhibition

Compound **7b** was further evaluated in an enzyme kinetic study. The kinetic inhibition data are summarised in Table 4 and the Lineweaver-Burk plot is shown in Figure 1. The calculated Michaelis constant ($K_m$) and maximal rate of reaction ($V_{max}$) for BChE inhibition increase when the concentration of compound **7b** increases from 0 to 3 µM. When it increases further to 6 µM, $K_m$ decreases and $V_{max}$ remains unchanged. At 12 µM inhibitor concentration, both $K_m$ and $V_{max}$ values decline. Lineweaver-Burk plot is a reciprocal reaction velocity (1/V) versus reciprocal substrate concentration (1/[S]) graph for inhibitors at different concentrations. The plot shows an intercept occurring above the x-axis at increasing concentration of the inhibitor, suggesting mixed-mode inhibition [38]. The findings indicate that compound **7b** is a mixed-mode inhibitor of BChE, where it can bind to the enzyme's active or allosteric sites. The binding of an inhibitor to the enzyme active site prevents the insertion and breakdown of butyrylthiocholine. In contrast, an inhibitor binding to allosteric sites may alter the shape of the enzyme, making it no longer optimal to accommodate butyrylthiocholine in its active site [39]. Mixed-mode inhibition is a special case that can have both competitive and non-competitive traits. A recent study reported a BChE inhibitor, norcymserine, suppresses the breakdown of acetylcholine in the post-mortem AD brain [40]. Spiropyrrolidine compounds could potentially be good alternatives for AD patients not responding to selective AChE inhibitors.

**Table 4** Kinetic parameters of butyrylcholinesterase (BChE) inhibition for compound **7b**.

| **Concentration (µM)** | $K_m$ **(mM)** | $V_{max}$ **(ΔOD412/min)** |
|---|---|---|
| 0 (no inhibitor) | 13.54 ± 2.28 | 0.066 ± 0.012 |
| 3 | 21.46 ± 9.04 | 0.077 ± 0.016 |
| 6 | 17.32 ± 7.65 | 0.077 ± 0.032 |
| 12 | 31.57 ± 13.25 | 0.077 ± 0.012 |

All data are presented as mean ± standard error, SE (n=3).

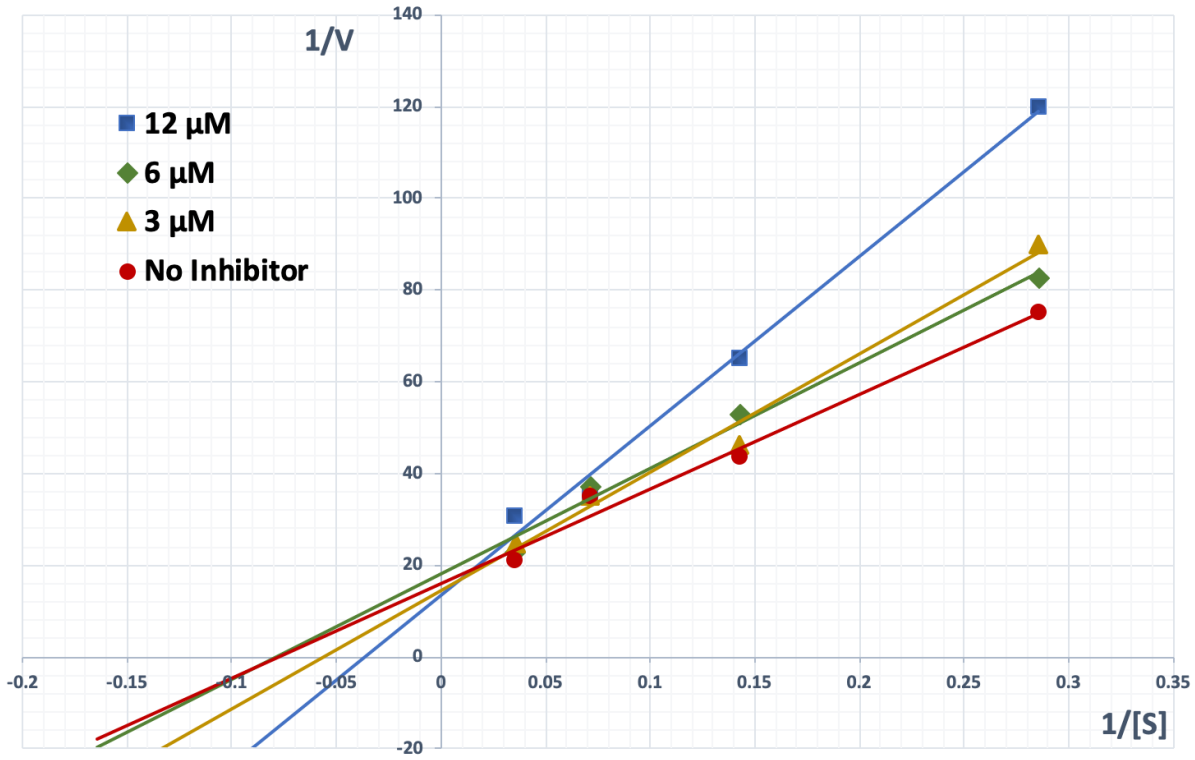


**Figure 1** Lineweaver-Burk plot of butyrylcholinesterase (BChE) inhibition of compound **7b**.

### 3.4. Molecular docking studies

The free binding energy and interaction modes between compound **7b** and residues in the active site of either human BChE or human AChE were identified by molecular docking studies using AutoDock Vina version 1.14. The crystal structures of human BChE complexed with thioflavin T (PDB ID: 6ESY) and human AChE complexed with dihydrotanshinone 1 (PDB ID: 4M0E) were used as a reference structure for the docking process [41-42].

Since **7b** had been prepared as a racemic mixture and used as such in the biological assays, calculations were carried out with both enantiomers of the molecule. For the enantiomer (*S*,*S*,*R*)-**7b**, having the same absolute configuration as drawn in Schemes 1-2 and Tables 1-2, the docking results indicated binding energies of –13.9 and –9.7 kcal $mol^{-1}$ for BChE and AChE, respectively (Table 5). For the other enantiomer, (*R*,*R*,*S*)-**7b**, these binding energies were calculated to be −12.0 kcal $mol^{-1}$ for BChE and −8.6 kcal $mol^{-1}$ for AChE. These results are fully consistent with the experimentally observed higher inhibitory activity of **7b** against BChE

than against AChE. Moreover, they suggest that (*S*,*S*,*R*)-**7b** is a significantly better inhibitor towards both enzymes than its enantiomer (*R*,*R*,*S*)-**7b**. To ascertain this, separation or enantioselective synthesis of these enantiomers would be required, in order to evaluate their individual activities. This may be done on the occasion of future studies.

**Table 5** Binding energies between butyrylcholinesterase or acetylcholinesterase with both enantiomers of compound **7b** and control (Thioflavin T; TFX or Dihydrotanshinone 1; 1YL), respectively

| Enzyme | Compound | Binding energy (kcal $mol^{-1}$) |
|---|---|---|
| Butyrylcholinesterase (PDB 6ESY) | (*S*,*S*,*R*)-**7b** | −13.9 ± 0.11 |
| | (*R*,*R*,*S*)-**7b** | −12.0 ± 0.00 |
| | TFX | −7.8 ± 0.26 |
| Acetylcholinesterase (PDB 4M0E) | (*S*,*S*,*R*)-**7b** | −9.7 ± 0.12 |
| | (*R*,*R*,*S*)-**7b** | −8.6 ± 0.23 |
| | 1YL | −7.5 ± 0.17 |

All data are presented as mean ± standard error, SE (n=3).

Interaction modes of both enantiomers of compound **7b** with BChE residues are shown in Figure 2, and details of their interaction in the active sites are listed in Table 6. The binding interactions of (*S*,*S*,*R*)-**7b** in BChE (Figure 2, left) show seven hydrophobic interactions between all three of phenyl groups and amino acids residue TYR332, TRP82, PHE329, GLY116, TRP231, LEU 286 and GLY117. The result explained that the oxindole NH group and pyrrolidine CH played an important role in the binding interaction and beneficial role of the amino acid residue ASP70 and THR120 via hydrogen bond. The bromine also shows hydrophobic interaction with HIS438 and TRP82. As displayed in Figure 2 (right) and Table 6, the enantiomer (*R*,*R*,*S*)-**7b** is the subject of hydrophobic interactions between TYR332,

TRP82, TRP231 and LEU286 with three phenyl rings. One anionic interaction was observed at phenyl group with ASP70. No other interaction was observed in oxindole. Based on this molecular docking result, we can conclude that the isatin ring played a huge contribution in inhibiting the BChE enzyme and interaction with the amino acid residue via hydrogen bond.

Interaction of the active molecules with these residues may block the catalysis process of BChE against its substrate, butyrylthiocholine. The docking analysis suggests that if the active molecules bind competitively with the substrate in the active pocket, both enantiomers of **7b** are able to interact with the P-site and the A-site of the enzyme (TYR322, TRP82, TRP231 and PHE329), mostly via hydrophobic interaction. Since both sites are crucial for substrate activation, inhibition of the enzyme by interactions of potential inhibitors with this pocket are promising. In addition, the interactions that formed between ASP70 with molecule (*S*,*S*,*R*)-**7b**, viewed from docking analysis suggested to eliminate substrate activation in BChE by blocking the hydrogen bond formation between ASP70 with TYR322 [41]. The molecules may comprise the mode of actions like most of the inhibitors against BChE.

**Table 6** Binding interactions between both enantiomers of compound **7b** and butyrylcholinesterase (BChE)

| Compound | Interacting unit | Protein residue | Type of interaction |
|---|---|---|---|
| (*S*,*S*,*R*)-**7b** | CH | ASP70 | H-bond |
| | NH | THR120 | H-bond |
| | Br | HIS438 | π-alkyl |
| | Br | TRP82 | π-π stacked |
| | Ph | TYR332 | π-π stacked |
| | Ph | TRP82 | π-π stacked |
| | Ph | PHE329 | π-π stacked |
| | Ph | GLY116 | π-π stacked |
| | Ph | TRP231 | π-π stacked |
| | Ph | LEU286 | π-alkyl |
| | Ph | GLY117 | Van der Waals |
| (*R*,*R*,*S*)-**7b** | Ph | ASP70 | π-anion |
| | Ph | TYR332 | π-π stacked |
| | Ph | TRP82 | π-π stacked |
| | Ph | TRP231 | π-π stacked |
| | Ph | LEU286 | π-alkyl |

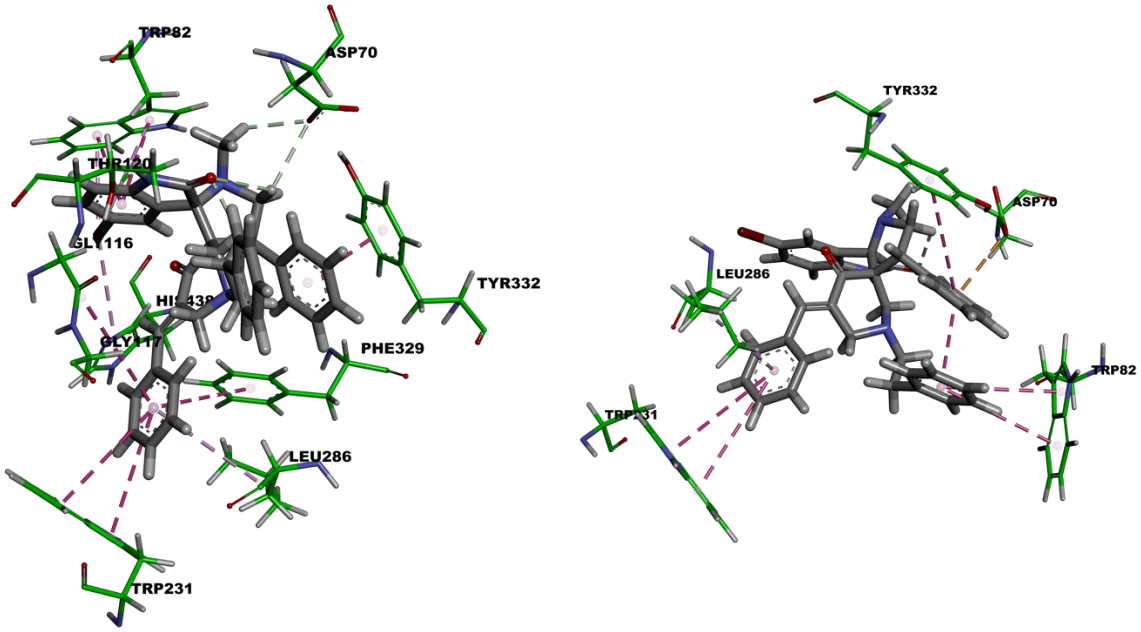


**Figure 2** Three-dimensional binding modes of enantiomer (*S*,*S*,*R*)-**7b** (left) and enantiomer (*R*,*R*,*S*)-**7b** (right) in the active site of BChE

## 3. Conclusions

In summary, new dispiropyrolidine derivatives were synthesised by a facile one-pot, three-component [3+2]-cycloaddition protocol. The designed new cycloadducts were screened for their inhibitory activities against cholinesterase enzymes. The inhibitory activities exhibited by the tested compounds were typically higher against BChE than AChE. Compound **7b** displayed a moderate BChE inhibitory activity, with an $IC_{50}$ of 12.78 ± 1.52 μM. Kinetic studies showed that **7b** is a mixed-mode inhibitor. It can be projected from the present study that the dispiro pyrrolidine **7b** could be further modified to improve its potential as a potent BChE selective inhibitor.

## 4. Materials and method

### 4.1. General

All chemicals reagents were obtained from Acros Organic (USA), QRec (Asia), Sigma Aldrich Chemical Co. and E. Merck (Germany). Melting points were determined on a Stuart Scientific SMP10 or SMP40 melting point apparatus. Thin-layer chromatography (TLC) plates was performed on alumina plates pre-coated with silica gel (Merck 60 F254) in the solvent system acetone-hexane with two different ratios of 3:7 or 1:9. The progress of reactions was determined by the appearance of product and disappearance of reactant spots under UV radiation lamp ($\lambda_{max}$ = 254 nm), respectively. All spectral data were obtained on the following instruments: infrared spectra were recorded on a Perkin Elmer 2000 FTIR spectrometer at wavenumbers ranging from 4000 to 600 $cm^{-1}$. $^{1}H$ (400.2 or 500 MHz) and $^{13}C$ (100.6 or 125 MHz) nuclear magnetic resonance spectra were recorded with an AVANCE 400 or an AVN 500 Bruker spectrometer (Bruker Biospin, Billerica, MA, U.S.A.). Data were analysed using NMRnotebook 2.80 (NMRTEC S.A.S.). Chemical shifts $\delta$ are reported in parts per million

(ppm), referenced to the peak of tetramethylsilane, defined at $\delta$ = 0.00 ($^{1}$H and $^{13}$C NMR), or the residual solvent peak, defined at $\delta$ = 2.50 ($^{1}$H NMR, DMSO-$d_6$), 7.26 ($^{1}$H NMR, $CDCl_3$), 39.5 ($^{13}$C NMR, DMSO-$d_6$) or 77.0 ($^{13}$C NMR, $CDCl_3$). Multiplicities are abbreviated as follows: s (singlet), d (doublet), t (triplet), q (quartet), quint (quintet), m (multiplet), br (broad). Coupling constants *J* are given in Hz and are rounded to the closest multiple of 0.5. Mass spectrometry experiments were performed using a Waters Xevo QTOF MS system or, alternatively, on a tims-TOF mass spectrometer (Bruker) in the *Laboratoire de Chimie Moléculaire* (Ecole polytechnique, CNRS, Palaiseau, France). The electrospray source was used in positive mode. Samples were prepared in acetonitrile with 0.1% of formic acid, introduced at a 5 μL/min flow rate into the interface of the instrument. Capillary and end plate voltages were set at 4.5 kV and 0.7 kV. Nitrogen was used as the nebulizer and drying gas at 2.5 bar and 3 L/min, respectively, with a drying temperature of 180°C. Tuning mix (Agilent) was used for calibration. The elemental compositions of all ions were determined with the instrument software Data Analysis; the precision of mass measurement was less than 3 ppm.

For the assays the chemicals and enzymes used in the cholinesterase inhibition investigation are as follows: Acetylthiocholine iodide (Sigma Aldrich, USA); 5,5'-Dithiobis-2-benzoic acid (Sigma Aldrich, USA); Acetylcholinesterase (AChE) from Electrophorus electricus (electric eel) (Sigma Aldrich, USA); Butyrylthiocholine iodide (Sigma Aldrich, USA); Butyrylcholinesterase (BChE) from equine serum (Sigma Aldrich, USA).

### 4.2. Chemistry

#### 4.2.1. General procedure for synthesis of (3E,5E)-3,5-bis(arylidene)-1-phenethyl-4-piperidinone (**3-4**)

The intermediate compounds, 3,5-bis(arylidene)-1-phenylethyl-4-piperidones (**3-4**) were synthesised following the synthesis protocol reported in the literature [24]. A mixture of

1-phenylethyl-4-piperidone **1** (1.00 mmol) and appropriate aryl aldehyde **2** (2.00 mmol) was dissolved in ethanol (10 mL) and 30% sodium hydroxide (5.0 mL) and stirred for 2-6 hours at room temperature until completion of the reaction (as evidenced by TLC). The mixture was then poured onto crushed ice. The solid precipitate was filtered off and washed with water to afford the product, which was then purified by recrystallisation.

4.2.1.1 3,5-Dibenzylidene-1-phenylethyl-4-piperidinone (**3**)

Yellow crystals. $R_f$ ≈ 0.2 [UV-active, EtOAc/petroleum ether 20%, orange spot (anisaldehyde)]. M.p. 88−92 ˚C (EtOH) (Lit. 165 °C) [24]. FTIR (ATR, neat): *v* 3026 (w, C-H), 1669 (s, C=O), 1608 (s, C=C), 1181 (m, C-N) $cm^{-1}$. $^1$H NMR (400 MHz, $CDCl_3$): *δ* 2.74 (2H, m), 2.81 (2H, m), 3.90 (4H, d, *J*= 1.5), 7.11 (2H, dd, *J* =8.0, 1.5), 7.15 (1H, tt, *J*= 7.5, 1.5), 7.23 (2 H, br dd, *J*= 8.0, 7.5), 7.34-7.46 (10H, m), 7.83 (2H, t, *J*= 1.5). $^{13}$C NMR (100.6 MHz, $CDCl_3$): *δ* 34.0 (C2), 54.7 (C7), 58.6 (C1), 126.1 (C6), 128.4 (C4), 128.6 (C5), 128.6 (C13), 129.0 (C14), 130.4 (C12), 133.2 (C8), 135.2 (C11), 136.7 (C10), 139.8 (C3), 187.4 (C9). $^1$H NMR (500 MHz, DMSO-$d_6$): *δ* 2.70 (2H, t, *J*= 7.5), 2.81 (2H, t, *J*= 7.5), 3.88 (4H, s), 7.14-7.23 (5H, m), 7.42-7.51 (10H, m), 7.58 (2H, s). $^{13}$C NMR (125.8 MHz, DMSO-$d_6$): *δ* 32.8 (C2), 54.0 (C7), 57.8 (C1), 125.8 (C6), 128.1 (C4), 128.5 (C5), 128.7 (C13), 129.2 (C14), 130.5 (C12), 133.8 (C8), 134.6 (C11), 134.8 (C10), 140.0 (C3), 186.9 (C9). HRMS (TOF-ES$^+$): *m/z* 380.2016 ($MH^+$ $C_{27}H_{26}NO^+$ requires 380.2009).

4.2.1.2 3,5-Bis(4-methylbenzylidene)-1-phenylethyl-4-piperidinone (**4**)

Yellow solid. $R_f$ ≈ 0.78 [UV-active, Acetone:hexane 10%]. M.p. 118−121 ˚C. FTIR (ATR, neat): *v* 3024 (w, C−H), 1668 (s, C=O), 1606 (m, C=C), 1175 (m, C−N) $cm^{-1}$. $^1$H NMR (500 MHz, DMSO-$d_6$): *δ* 2.35 (6H, s), 2.70 (2H, distorted t, *J*= 7.5), 2.80 (2H, distorted t, *J*= 7.5), 3.85 (4H, br s), 7.14 (1H, tt, *J*= 7.5, 1.5), 7.15 (2H, d, *J* =7.5), 7.22 (2H, br t, *J*= 7.5), 7.28

(4H, d, *J*= 8.0), 7.39 (4H, d, *J*= 8.0), 7.57 (2H, br s). $^{13}$C NMR (125.8 MHz, DMSO-$d_6$): $\delta$ 21.0 (C15), 32.8 (C2), 54.1 (C7), 57.9 (C1), 125.8 (C6), 128.2 (C4), 128.5 (C5), 129.4 (C13), 130.5 (C12), 131.9 (C11), 133.0 (C8), 134.7 (C10), 139.1 (C14), 140.0 (C3), 186.8 (C9). HRMS (TOF-ES$^+$): *m/z* 408.2324 ($MH^+$ $C_{29}H_{30}NO^+$ requires 408.2322).

4.2.2. General procedure for synthesis of spiropyrrolidines derivatives **7a-h**

(3*E*,5*E*)-3,5-Bis(arylidene)-1-phenethyl-4-piperidinone **3** or **4** (1.50 mmol) was refluxed together with the appropriate isatin **5a-d** (1.50 mmol) and sarcosine **6** (3.00 mmol) in methanol (20 mL) for 4-7 hours. After completion of the reaction, the mixture was allowed to cool to room temperature. Most of the solvent was removed under reduced pressure and the residue was poured onto crushed ice. The solid product obtained was filtered off and washed with water. In some cases, further purification by recrystallisation was carried out.

4.2.2.1 1-Methyl-4(phenyl)pyrrolo-(spiro[2.3'']oxindole)-spiro[3.3']-5'-(phenylmethylidene)-1'-phenylethyl-4'-piperidinone (**7a**)

Pale yellow crystal. $R_f \approx 0.15$ [UV-active, EtOAc:petroleum ether 20%]. M.p. 200-202 ˚C. $^1$H NMR (400 MHz, $CDCl_3$): $\delta$ 1.73 (1H, d, *J*=12.5), 2.07 (3H, s), 2.34 (1H, ddd, *J*= 12.0, 6.5, 5.0), 2.53 (2H, AB part of an ABXY system, $\delta_A$ 2.48, $\delta_B$ 2.57, $J_{AB}$= 14.0, $J_{AX}$= 6.5, $J_{AY}$= 9.0, $J_{BX}$= 5.0, $J_{BY}$= 7.0), 2.78 (ddd, *J*= 12.0, 9.0, 7.0), 2.78 (1H, dd, *J*= 14.0, 2.0), 3.25 (1H, dd, *J*= 8.5, 7.0), 3.34 (1H, dd, *J*= 12.5, 2.0), 3.65 (1H, ddd, *J*= 14.5, 2.0, 1.5), 3.88 (1H, dd, *J*= 11.5, 8.5), 4.80 (1H, dd, *J*= 11.5, 7.0), 6.04 (1H, br s, NH), 6.38 (1H, br d, *J*= 7.5), 6.93 (1H, td, *J*= 7.5, 1.0), 6.97 (1H, dd, *J*= 2.0, 1.5), 6.98 (2H, br dd, *J*= 7.5, 2.0), 7.01 (2H, br dd, *J*= 8.0, 1.5), 7.05 (1H, br dd, *J*= 7.5, 1.5), 7.07 (1H, ddd, *J*= 8.0, 7.5, 1.5), 7.20-7.34 (9H, m), 7.37 (2H, br dd, *J*= 7.5, 1.5). $^{13}$C NMR (100.6 MHz, $CDCl_3$): $\delta$ 32.5 (C2), 34.6 (C22), 45.6 (C12), 53.4 (C7), 56.2 (C13), 57.0 (C11), 58.8 (C1), 66.1 (C10), 75.0 (C14), 108.7 (C19), 121.7 (C17), 125.8

(C6), 126.7 (C26), 127.5 (C15), 127.6 (C16), 128.17, 128.19 (C4, C25), 128.3, 128.5 (C5, C30), 129.0 (C18), 129.0 (C31), 129.3 (C24), 129.8 (C29), 133.5 (C8), 135.2 (C28), 137.5 (C27), 138.3 (C23), 140.8 (C3), 141.9 (C20), 176.7 (C21), 198.9 (C9). $^{1}$H NMR (500 MHz, DMSO-$d_6$): $\delta$ 1.76 (1H, d, *J*=12.5), 1.99 (3H, s), 2.30−2.55 (4H, m), 3.06 (1H, dd, *J*= 15.0, 2.5), 3.21 (1H, dd, *J*= 8.5, 7.5), 3.23 (1H, d, *J*= 12.5), 3.34 (1H, br d, *J*= 15.0), 3.83 (1H, dd, *J*= 11.0, 8.5), 4.65 (1H, dd, *J*= 11.0, 7.5), 6.64 (1H, br d, *J*= 7.5), 6.85−6.90 (2H, m), 7.05 (1H, ddd, *J*= 7.5, 6.0, 2.5), 7.09 (1H, m), 7.11 (2H, d, *J*= 7.5), 7.11 (2H, d, *J*= 7.0), 7.11 (1H, t, *J*= 7.0), 7.15 (1H, br t, *J*= 7.5), 7.22 (2H, dd, *J*= 7.5, 7.0), 7.30−7.36 (7H, m), 10.38 (1H, br s, NH). $^{13}$C NMR (125.8 MHz, DMSO-$d_6$): $\delta$ 32.0 (C2), 34.1 (C22), 45.2 (C12), 53.9 (C7), 56.2, 56.3 (C11, C13), 59.1 (C1), 64.6 (C10), 75.2 (C14), 108.7 (C19), 120.7 (C17), 125.8 (C6), 126.75 (C16 or C26), 126.85 (C15), 126.91 (C16 or C26), 128.18 128.20 (C4, C25), 128.46, 128.47 (C5, C30), 128.6 (C18), 128.9 (C31), 129.1 (C24), 130.0 (C29), 132.9 (C8), 134.5 (C28), 136.6 (C27), 138.4 (C23), 140.0 (C3), 143.4 (C20), 176.6 (C21), 198.2 (C9). HRMS (TOF-ES$^{+}$): *m/z* 554.2801 ($MH^{+}$ $C_{37}H_{36}N_3O_2^{+}$ requires 554.2802).

4.2.2.2 1-Methyl-4(phenyl)pyrrolo-(spiro[2.3"]-5"-bromooxindole)-spiro[3.3']-5'-(phenylmethylidene)-1'-phenylethyl-4'-piperidinone (**7b**)

Pale yellow solid. $R_f \approx 0.62$ [UV-active, Acetone:hexane 10%]. M.p. 123-126 ˚C. FTIR (ATR, neat): $\nu$ 3387 (w, N−H), 3026 (w, C−H), 1711 (s, C=O), 1614 (m, C=C), 1181 (m, C−N) $cm^{-1}$. $^{1}$H NMR (500 MHz, DMSO-$d_6$): $\delta$ 1.75 (1H, d, *J*= 12.5), 2.01 (3H, s), 2.32−2.53 (4H, m), 3.10 (1H, dd, *J*= 15.0, 3.0), 3.22 (1H, dd, *J*= 8.5, 7.5), 3.22 (1H, dd, *J*= 12.5, 1.5), 3.38 (1H, br d, *J*= 15.0), 3.81 (1H, dd, *J*= 11.0, 8.5), 4.64 (1H, dd, *J*= 11.0, 7.5), 6.61 (1H, d, *J*= 8.0), 6.94 (1H, d, *J*= 2.0), 7.11 (2H, br d, *J*= 7.5), 7.12 (1H, t, *J*= 7.5), 7.13 (1H, m), 7.14 (1H, t, *J*= 7.5), 7.19 (2H, dd, *J*= 8.0, 2.0), 7.23 (2H, t, *J*= 7.5), 7.24 (1H, dd, *J*= 8.0, 2.0), 7.30−7.38 (7H, m), 10.56 (1H, br s, NH). $^{13}$C NMR (125.8 MHz, DMSO-$d_6$): $\delta$ 31.8 (C2), 34.1 (C22), 45.0

(C12), 53.9 (C7), 56.2, 56.3 (C11, C13), 59.0 (C1), 65.0 (C10), 75.0 (C14), 110.7 (C19), 112.6 (C17), 125.8 (C6), 126.8 (C26), 128.16 (C4), 128.24 (C25), 128.4 (C5), 128.5 (C30), 129.08 (C24), 129.10 (C31), 129.4 (C15), 129.5 (C16), 130.0 (C29), 131.2 (C18), 133.0 (C8), 134.3 (C28), 137.0 (C27), 138.1 (C23), 139.9 (C3), 142.7 (C20), 176.0 (C21), 198.1 (C9). HRMS (TOF-ES$^-$) *m/z* 630.0966 ([M−H]$^-$ $C_{37}H_{33}{}^{79}BrN_3O_2^-$ requires 630.1761), 632.0932 ([M−H]$^-$ $C_{37}H_{33}{}^{81}BrN_3O_2^-$ requires 632.1741).

4.2.2.3 1-Methyl-4(phenyl)pyrrolo-(spiro[2.3"]-5"-chlorooxindole)-spiro[3.3']-5'-(phenylmethylidene)-1'-phenylethyl-4'-piperidinone (**7c**)

Pale yellow solid. $R_f \approx 0.63$ [UV-active, Acetone:hexane 10%]. M.p. 131-134 ˚C. FTIR (ATR, neat): *v* 3244 (w, N−H), 3027 (w, C−H), 1698 (s, C=O), 1615 (m, C=C), 1182 (m, C−N) cm$^{-1}$. $^1$H NMR (500 MHz, DMSO-d$_6$): *δ* 1.75 (1H, d, *J*= 12.5), 2.01 (3H, s), 2.32−2.53 (4H, m), 3.10 (1H, dd, *J*= 15.0, 2.5), 3.23 (1H, dd, *J*= 8.5, 7.5), 3.23 (1H, dd, *J*= 12.5, 1.5), 3.38 (1H, br d, *J*= 15.0), 3.81 (1H, dd, *J*= 11.0, 8.5), 4.65 (1H, dd, *J*= 11.0, 7.5), 6.66 (1H, d, *J*= 8.0), 6.82 (1H, d, *J*= 2.0), 7.11 (2H, br d, *J*= 7.5), 7.12 (1H, dd, *J*= 8.0, 2.0), 7.14 (1H, m), 7.15 (1H, t, *J*= 7.5), 7.13-7.18 (3H, m), 7.23 (2H, t, *J*= 7.5), 7.30−7.38 (7H, m), 10.56 (1H, s, NH). $^{13}$C NMR (125.8 MHz, DMSO-d$_6$): *δ* 32.0 (C2), 34.2 (C22), 45.1 (C12), 54.0 (C7), 56.3, 56.4 (C11, C13), 59.1 (C1), 65.1 (C10), 75.2 (C14), 110.3 (C19), 125.0 (C17), 125.9 (C6), 126.8 (C26), 126.9 (C16), 128.27 (C4), 128.34 (C25), 128.5 (C5), 128.6 (C18), 128.7 (C30), 129.1 (C15), 129.23 (C31), 129.1 (C15), 130.1 (C29), 133.1 (C8), 134.3 (C28), 137.2 (C27), 138.1 (C23), 140.0 (C3), 142.4 (C20), 176.3 (C21), 198.2 (C9). HRMS (TOF-ES$^+$): *m/z* 588.2390 (MH$^+$ $C_{37}H_{35}{}^{35}ClN_3O_2^+$ requires 588.2413).

4.2.2.4 1-Methyl-4(phenyl)pyrrolo-(spiro[2.3"]-5"-nitrooxindole)-spiro[3.3']-5'-(phenylmethylidene)-1'-phenylethyl piperidin-4'-one (**7d**)

Dark brown solid. $R_f$ ≈ 0.47 [UV-active, Acetone:hexane 10%]. M.p. 127−130 ˚C. FTIR (ATR, neat): *v* 3248 (w, N−H), 3026 (w, C−H), 1718 (s, C=O), 1599 (m, C=C), 1182 (m, C−N) $cm^{-1}$. $^1H$ NMR (500 MHz, DMSO-$d_6$): $\delta$ 1.76 (1H, d, *J*= 12.5), 2.03 (3H, s), 2.35−2.52 (4H, m), 3.11 (1H, dd, *J*= 15.0, 2.5), 3.19 (1H, dd, *J*= 12.5, 1.5), 3.29 (1H, dd, *J*= 8.5, 7.5), 3.35 (1H, br d, *J*= 15.0), 3.81 (1H, dd, *J*= 10.5, 8.5), 4.71 (1H, dd, *J*= 10.5, 7.5), 6.86 (1H, d, *J*= 8.5), 6.98 (2 H, m), 7.12 (2H, d, *J*= 7.0), 7.14 (1H, m), 7.14 (1H, t, *J*= 8.0), 7.15 (1H, t, *J*= 8.0), 7.23 (2H, dd, *J*= 8.0, 7.0), 7.31−7.35 (7H, m), 7.71 (1H, d, *J*= 2.5), 8.04 (1H, dd, *J*= 8.5, 2.5), 11.22 (1H, br s, NH). $^{13}C$ NMR (125.8 MHz, DMSO-$d_6$): $\delta$ 31.9 (C2), 34.2 (C22), 44.7 (C12), 53.8 (C7), 56.2, 56.5 (C11, C13), 59.0 (C1), 65.3 (C10), 75.0 (C14), 109.1 (C19), 122.6 (C16), 125.9 (C6), 126.1 (C18), 127.0 (C26), 127.8 (C15), 128.2 (C4), 128.36 (C25), 128.44 (C5), 128.7 (C30), 129.1 (C24), 129.3 (C31), 129.9 (C29), 132.8 (C8), 134.0 (C28), 137.3 (C27), 137.8 (C23), 139.8 (C3), 141.5 (C17), 150.0 (C20), 176.9 (C21), 197.7 (C9). HRMS (TOF-$ES^+$): *m/z* 599.2764 ($MH^+$ $C_{37}H_{35}N_4O_4^+$ requires 599.2653).

4.2.2.5 1-Methyl-4(-4-methylphenyl)pyrrolo-(spiro[2.3"]oxindole)-spiro[3.3']-5'-(4-methylphenylmethylidene)-1'-phenylethyl-4'-piperidinone (**7e**)

Pale yellow solid. $R_f$ ≈ 0.40 [UV-active, Acetone:hexane 10%]. M.p. 192−195 ˚C. FTIR (ATR, neat): *v* 3397 (w, N−H), 3023 (w, C−H), 1694 (s, C=O, 1605 (m, C=C), 1177 (m, C−N) $cm^{-1}$. $^1H$ NMR (500 MHz, DMSO-$d_6$): $\delta$ 1.76 (1H, d, *J*= 12.5), 1.98 (3H, s), 2.26 (3H, s), 2.27 (3H, s), 2.28−2.55 (4H, m), 3.04 (1H, dd, *J*= 15.0, 2.5), 3.16 (1H, dd, *J*= 8.5, 7.5), 3.20 (1H, dd, *J*= 12.5, 1.5), 3.33 (1H, dd, *J*= 15.0, 2.0), 3.79 (1H, dd, *J*= 11.0, 8.5), 4.60 (1H, dd, *J*= 11.0, 7.5), 6.63 (1H, br d, *J*= 7.5), 6.82−6.89 (2H, m), 7.01 (2H, d, *J*= 8.0), 7.03 (1H, ddd, *J*= 7.5, 7.0, 2.0), 7.06 (1H, dd, *J*= 2.5, 2.0), 7.11 (2H, br d, *J*= 8.0), 7.12 (2H, br d, *J*= 7.0), 7.14

(2H, br d, *J*= 8.0), 7.15 (1H, t, *J*= 8.0), 7.19 (2H, br d, *J*= 8.0), 7.23 (2H, dd, *J*= 8.0, 7.0), 10.35 (1H, br s, NH). $^{13}$C NMR (125.8 MHz, DMSO-$d_6$): $\delta$ 20.6 (C27), 20.9 (C33), 32.1 (C2), 34.1 (C22), 44.8 (C12), 54.0 (C7), 56.3, 56.4 (C11, C13), 59.1 (C1), 64.5 (C10), 75.2 (C14), 108.6 (C19), 120.6 (C17), 125.8 (C6), 126.88 (C16), 126.93 (C15), 128.2 (C4), 128.5 (C18), 128.4 (C5), 128.8 (C25), 129.0 (C31), 129.1 (C24), 130.2 (C30), 131.7 (C29), 132.1 (C8), 135.3 (C23), 135.7 (C26), 136.6 (C28), 138.8 (C32), 140.1 (C3), 143.4 (C20), 176.6 (C21), 198.2 (C9). HRMS (TOF-ES$^+$): *m/z* 582.3081 ($MH^+$ $C_{39}H_{40}N_3O_2^+$ requires 582.3115), 604.2894 ($MNa^+$ $C_{39}H_{39}N_3NaO_2^+$ requires 604.2935).

4.2.2.6 1-Methyl-4(-4-methylphenyl)pyrrolo-(spiro[2.3'']-5''-bromooxindole)-spiro[3.3']-5'-(4-methylphenylmethylidene)-1'-phenylethyl-4'-piperidinone (**7f**)

Pale yellow solid. $R_f$ ≈ 0.66 [UV-active, Acetone:hexane 10%]. M.p. 205−208 ˚C. FTIR (ATR, neat): *v* 3347 (w, N−H), 3024 (w, C−H), 1690 (s, C=O), 1604 (m, C=C), 1180 (m, C−N) cm$^{-1}$. $^1$H NMR (500 MHz, DMSO-$d_6$): $\delta$ 1.75 (1H, d, *J*= 12.5), 2.00 (3H, s), 2.26 (3H, s), 2.29 (3H, s), 2.29−2.53 (4H, m), 3.08 (1H, dd, *J*= 15.0, 2.5), 3.17 (1H, dd, *J*= 8.5, 7.0), 3.19 (1H, dd, *J*= 12.5, 1.5), 3.37 (1H, br d, *J*= 15.0), 3.76 (1H, dd, *J*= 11.0, 8.5), 4.59 (1H, dd, *J*= 11.0, 7.0), 6.60 (1H, d, *J*= 8.0), 6.92 (1H, d, *J*= 2.0), 7.09 (2H, d, *J*= 8.0), 7.09-7.12 (1H, m), 7.12 (2H, br d, *J*= 7.0), 7.12 (2H, br d, *J*= 8.0), 7.15 (1H, t, *J*= 8.0), 7.17 (2H, br d, *J*= 8.0), 7.18 (2H, br d, *J*= 8.0), 7.22 (1H, dd, *J*= 8.0, 2.0), 7.23 (2H, dd, *J*= 8.0, 7.0), 10.54 (1H, br s, NH). $^{13}$C NMR (125.8 MHz, DMSO-$d_6$): $\delta$ 20.7 (C27), 20.9 (C33), 32.0 (C2), 34.2 (C22), 44.7 (C12), 54.1 (C7), 56.351, 56.430 (C11, C13), 59.1 (C1), 65.0 (C10), 75.1 (C14), 110.7 (C19), 112.6 (C17), 125.9 (C6), 128.2 (C4), 128.5 (C5), 128.9 (C25), 129.0 (C31), 129.2 (C24), 129.6, 129.6 (C15, C16), 130.2 (C30), 131.2 (C18), 131.6 (C29), 132.2 (C8), 135.0 (C23), 135.9 (C26), 137.2 (C28), 139.2 (C32), 140.0 (C3), 142.7 (C20), 176.1 (C21), 198.0 (C9). HRMS

(TOF-ES$^+$): *m/z* 660.2328 ($MH^+$ $C_{39}H_{39}{}^{79}BrN_3O_2^+$ requires 660.2221), 662.2327 ($MH^+$ $C_{39}H_{39}{}^{81}BrN_3O_2^+$ requires 662.2200).

4.2.2.7 1-Methyl-4(-4-methylphenyl)pyrrolo-(spiro[2.3"]-5"-chlorooxindole)-spiro[3.3']-5'-(4-methylphenylmethylidene)-1'-phenylethyl-4'-piperidinone (**7g**)

Pale yellow solid. $R_f$ ≈ 0.66 [UV-active, Acetone:hexane 10%]. M.p. 186−189 ˚C. FTIR (ATR, neat): *v* 3180 (w, N−H), 3025 (w, C−H), 1691 (s, C=O), 1607 (m, C=C), 1182 (m, C−N) $cm^{-1}$. $^1$H NMR (500 MHz, DMSO-$d_6$): *δ* 1.75 (1H, d, *J*= 12.5), 2.00 (3H, s), 2.26 (3H, s), 2.29 (3H, s), 2.31−2.52 (4H, m), 3.08 (1H, dd, *J*= 15.0, 2.5), 3.18 (1H, dd, *J*= 8.5, 7.5), 3.20 (1H, dd, *J*= 12.5, 1.5), 3.37 (1H, br d, *J*= 15.0), 3.77 (1H, dd, *J*= 11.0, 8.5), 4.59 (1H, dd, *J*= 11.0, 7.5), 6.64 (1H, d, *J*= 8.5), 6.80 (1H, d, *J*= 2.0), 7.06 (2H, d, *J*= 8.0), 7.09 (1H, dd, *J*= 8.5, 2.0), 7.11 (1H, m), 7.12 (2H, br d, *J*= 7.0), 7.12 (2H, br d, *J*= 7.5), 7.15 (1H, t, *J*= 8.0), 7.17 (2H, br d, *J*= 8.0), 7.19 (2H, br d, *J*= 7.5), 7.23 (2H, dd, *J*= 8.0, 7.0), 10.53 (1H, br s, NH). $^{13}$C NMR (125.8 MHz, DMSO-$d_6$): *δ* 20.6 (C27), 20.9 (C33), 32.0 (C2), 34.1 (C22), 44.6 (C12), 54.0 (C7), 56.3, 56.4 (C11, C13), 59.0 (C1), 64.9 (C10), 75.2 (C14), 110.1 (C19), 124.8 (C17), 125.8 (C6), 126.8 (C16), 128.2 (C4), 128.3 (C18), 128.4 (C5), 128.8 (C25), 128.9 (C31), 129.1 (C15), 129.2 (C24), 130.1 (C30), 131.5 (C29), 132.2 (C8), 135.0 (C23), 135.8 (C26), 137.1 (C28), 139.1 (C32), 139.9 (C3), 142.3 (C20), 176.2 (C21), 198.1 (C9). HRMS (TOF-ES$^+$): *m/z* 616.2735 ($MH^+$ $C_{39}H_{39}{}^{35}ClN_3O_2^+$ requires 616.2726), 638.2595 ($MNa^+$ $C_{39}H_{38}{}^{35}ClN_3NaO_2^+$ requires 638.2545).

4.2.2.8 1-Methyl-4(-4-methylphenyl)pyrrolo-(spiro[2.3"]-5"-nitrooxindole)-spiro[3.3']-5'-(4-methylphenylmethylidene)-1'-phenylethyl-4'-piperidinone (**7h**)

Dark yellow solid. $R_f$ ≈ 0.41 [UV-active, Acetone:hexane 10%]. M.p. 191−194 ˚C. FTIR (ATR, neat): *v* 3294 (w, N−H), 3028 (w, C−H), 1701 (s, C=O), 1601 (m, C=C), 1177 (m, C−N)

$cm^{-1}$. $^{1}H$ NMR (500 MHz, DMSO-$d_6$): $\delta$ 1.76 (1H, d, *J*= 12.5), 2.02 (3H, s), 2.27 (6H, br s), 2.34−2.53 (4H, m), 3.09 (1H, dd, *J*= 15.0, 2.5), 3.16 (1H, dd, *J*= 12.5, 1.5), 3.25 (1H, dd, *J*= 8.5, 7.5), 3.34 (1H, br d, *J*= 15.0), 3.77 (1H, dd, *J*= 11.0, 8.5), 4.66 (1H, dd, *J*= 11.0, 7.5), 6.84 (1H, d, *J*= 8.5), 6.89 (2H, d, *J*= 8.0), 7.11 (1H, m), 7.13 (2H, br d, *J*= 7.0), 7.13 (2H, br d, *J*= 8.0), 7.14 (2H, br d, *J*= 8.0), 7.16 (1H, t, *J*= 8.0), 7.20 (2H, br d, *J*= 8.0), 7.24 (2H, dd, *J*= 8.0, 7.0), 7.70 (1H, d, *J*= 2.5), 8.02 (1H, dd, *J*= 8.5, 2.5), 11.19 (1H, br s, NH). $^{13}C$ NMR (125.8 MHz, DMSO-$d_6$): $\delta$ 20.6, 20.9 (C27, C33), 31.9 (C2), 34.1 (C22), 44.3 (C12), 53.9 (C7), 56.2, 56.5 (C11, C13), 59.0 (C1), 65.2 (C10), 75.0 (C14), 109.0 (C19), 122.6 (C16), 125.9 (C6), 126.0 (C18), 127.9 (C15), 128.2 (C4), 128.4 (C5), 128.91, 128.95 (C25, C31), 129.3 (C24), 130.0 (C30), 131.9 (C29), 132.3 (C8) 134.7 (C23), 135.9 (C26), 137.3 (C28), 139.4 (C32), 139.8 (C3), 141.4 (C17), 149.9 (C20), 176.9 (C21), 197.7 (C9). HRMS (TOF-$ES^+$): *m/z* 627.3000 ($MH^+$ $C_{39}H_{39}N_4O_4^+$ requires 627.2966).

### 4.3. Biology

#### 4.3.1 Assay for Cholinesterase Inhibitions

4.3.1.1 Preparation of samples, reagents and enzyme solutions.

Physostigmine was used as a positive control. The test samples and physostigmine were initially prepared in dimethylsulfoxide (DMSO) solution at a concentration of 1 mg/mL. The reaction mixture was diluted with phosphate buffer until the concentration of DMSO was 10%. The concentration of DMSO in the reaction mixture was further diluted with the addition of reagents and enzyme solutions until the final reaction mixture was 1%. The concentration of DMSO of 1% gives no inhibitory effect towards both acetylcholinesterase and butyrylcholinesterase enzymes.

The 0.1 M phosphate buffer with pH 8.0 was used as an aqueous medium for enzymatic reaction in the cholinesterase inhibitory assay. The 0.01 M of dithiobisnitrobenzoic

acid (DTNB) was prepared by dissolved 39.6 mg of DTNB in 10 mL of phosphate buffer (pH 8.0). Two substrate solutions, acetylthiocholine iodide (AChI) and butyrylthiocholine iodide (BChI) were prepared at a concentration of 0.014 M by dissolving 40.4 mg of AChI and 31.6 mg of BChI respectively in 10 mL deionized water. Acetylcholinesterase (AChE) from electric eel and butyrylcholinesterase (BChE) from equine serum was used at a concentration of 0.09 u/mL enzyme solution in buffer pH 7.4 as enzyme working solution.

4.3.1.2 Ellman's Assay and $IC_{50}$ determination

The activities of AChE and BChE were conducted based on Ellman's method using a 96-wells microplate plate assay [26]. The reaction mechanism of this assay is based on the hydrolysis of AChI or BChI by AChE or BChE to thiocholine and acetate entities, respectively. Assay of acetylcholinesterase (AChE) activity was started by adding 140 µL of 0.1 M phosphate buffer (pH 8.0) into each well of a 96-well microplate. Test samples were added and followed with 20 µL of 0.09 u/mL acetylcholinesterase. The microplate was incubated for 15 minutes at 25 ˚C (in dark) before 10 µL of 10 mM DTNB were added into each well and followed with 10 µL of 14 mM acetylthiocholine iodide. The concentration of 10% DMSO in 20 µL reaction mixture was diluted to 1% DMSO with the addition of 140 µL reagents and enzyme solutions. BioTek PowerWave X 340 microplate spectrophotometer was used to measure the absorbance of the coloured end-product, 5-thio-2-nitrobenzoate at 412 nm after the enzymatic reaction initiated for 30 minutes. The BChE activity assay was conducted using the same procedure described above with different enzyme and substrate, butyrylthiocholine esterase from equine serum and butyryl-choline iodide.

Each test was performed in triplicate. The blank absorbance is the absorbance of test samples in DMSO with substrate and DTNB, but without enzyme. The test samples'

absorbance was corrected by subtracting the absorbance of their respective blank. The following formula was used to calculate the percentage of inhibition (Eq. 1)

$$\% \text{ Inhibition} = (\text{Abs. control} - \text{Abs. sample})/\text{Abs control} \times 100 \quad \text{(Eq. 1)}$$

Compound with more than 50% inhibition potential during the screening was further tested to determine the half-maximal inhibitory concentration ($IC_{50}$). The procedure was conducted using same procedure described above with enzyme butyrylcholine esterase from equine serum, butyrylthiocholine iodide as substrate and a set of five concentrations test sample, 1.25, 2.5, 5, 10, and 20 µM.

**4.3.2 Kinetic study and inhibition mode**

Determinations of enzyme kinetic and inhibition mode were done by using Lineweaver-Burk analysis. The Lineweaver-Burk or double-reciprocal plot (Eq. 2) is a reciprocal rearrangement of the Michaelis-Menten equation (Eq. 3) to give a linear dependent 1/v upon 1/[S] displaying the kinetic behaviour of the inhibitor.

$$v = ([S]V_{max}) / (K_m+[S]) \quad \text{(Eq. 2)}$$

$$1/v = (K_m/V_{max})(1/[S]) + (1/V_{max}) \quad \text{(Eq. 3)}$$

The enzyme inhibition kinetic was conducted in the absence and presence of sample compound at concentration of 0 µM, 3 µM, 6 µM and 12 µM at a different concentration of substrate 3.5 mM, 7 mM, 14 mM and 28 mM. Kinetic parameters of inhibition, Michealis-

Menten ($K_m$) constant and maximum velocity ($V_{max}$) were derived from Lineweaver-Burk plot [27].

### 4.3.4 Molecular docking

The three-dimensional coordinates of reference structure such as human butyrylcholinesterase, BChE complexed with Thioflavin T (PDB ID: 6ESY) and human acetylcholinesterase, AChE complexed with Dihydrotanshinone 1 (PDB ID: 4M0E) were fetched by ID from the Protein Data Bank (PDB) database in UCSF Chimera version 1.14 /1.15 [28]. Before docking, both crystal PDBs were processed using Dock Prep tool, starting by removing of water molecules and unrelated hetam, followed with separation of receptor and inhibitor from the complexes into individual structures and finally minimization of individual structures by steepest descent steps (polar hydrogens and Gasteiger charges were added) [29]. The two enantiomers of compound **7b** were built using ChemDraw and subsequently converted from cdx format to PDB.

To recognize the binding sites in BChE, the grid size was set to 65, 74, and 69 along the X-, Y-, and Z-axes with a 0.375Å grid spacing. The grid centre along the X-, Y-, Z-axes was set to -2, -9, and -15Å. Meanwhile, to recognize the binding sites in AChE, the grid size was set to 90, 81, and 74 along with the X-, Y-, and Z-axes with a 0.375Å grid spacing. The grid centre along the X-, Y-, Z-axes was set to 33, 46, and 131Å. The AutoDock Vina tool was finally used to calculate possible bindings and energies [30]. The output from AutoDock Vina was further analyzed using Biovia Discovery Studio Visualizer Client 2020 (Dassault Systèmes BIOVIA, Discovery Studio Modeling Environment, Release 2017, San Diego: Dassault Systèmes, 2016).

## Conflict of Interest

The authors declare no potential conflict of interest.

## Authors Contributions

**Nadia Mohamed Yusoff:** Methodology, Formal Analysis, Investigation, Data Curation, Writing–Original Draft Preparation, Visualization. **Hasnah Osman:** Conceptualization, Methodology, Resources, Supervision, Project Administration, Funding Acquisition. **Valentia Katemba:** Methodology, Formal Analysis, Investigation, Data Curation. **Muhammad Solehin Abd Ghani:** Formal Analysis, Investigation, Data Curation, Writing–Original Draft Preparation. **Unang Supratman:** Investigation, Data Curation, Writing–Review and Editing. **Mohammad Tasyriq Che Omar:** Software, Formal Analysis, Writing–Original Draft Preparation. **Vikneswaran Murugaiyah:** Methodology, Resources, Writing–Review and Editing, Supervision. **Xiang Ren:** Investigation, Data Curation. **Yvan Six:** Methodology, Validation, Writing–Original Draft Preparation, Writing–Review and Editing, Visualization. **Mohamad Nurul Azmi:** Conceptualization, Methodology, Validation, Resources, Writing–Original Draft Preparation, Writing–Review and Editing, Visualization, Supervision, Project Administration, Funding Acquisition. All authors have read and agreed to the published version of the manuscript.

## Declaration of Competing Interest

The authors declare that they have no known competing financial interests or personal relationships that could have appeared to influence the work reported in this paper.

**Acknowledgement**

We are grateful to the Malaysian Ministry of Education (MOHE), and the French Ministry of Europe and Foreign Affairs, the French Ministry of Higher Education, Research and Innovation for the PHC Hibiscus grant (Hubert Curien Partnership) MyPAIR/1/2019/STG01/USM/2. We also thank Universiti Sains Malaysia (USM) for research grants [RUI 1001.PKIMIA.8011072] to financially support this research and thank the Malaysian government for the scholarship (MyBrain15) (Mohamed Yusoff, N.).

**Appendix A. Supplementary data**

Supplementary data related to this article can be found at

**References**

1. L.K. Smith, I.R. Baxendale, Total Syntheses of Natural Products Containing Spirocarbocycles, Org. Biomol. Chem. 13 (2015) 9907–9933. https://doi.org/10.1039/C5OB01524C

2. A.J. Boddy, J.A. Bull, Stereoselective Synthesis and Applications of Spirocyclic Oxindoles. Org. Chem. Front. 8 (2021) 1026-1084. https://doi.org/10.1039/D0QO01085E

3. C.V. Galliford, K.A. Scheidt, Pyrrolidinyl-Spirooxindole Natural Products as Inspirations for The Development of Potential Therapeutic Agents. Angew. Chem. Int. Ed. 46 (2007) 8748–8758. https://doi.org/10.1002/anie.200701342

4. G. Molteni, A. Silvani, Spiro-2-oxindoles via 1,3-Dipolar Cycloaddition: A Decade Update, Eur. J. Org. Chem. 2021 (2021) 1653-1675. https://doi.org/10.1002/ejoc.202100121

5. A.S. Girgis, S.S. Panda, I.S. Ahmed Farag, A.M. El-Shabiny, A.M. Moustafa, N.S.M. Ismail, G.G. Pillai, C.S. Panda, C.D. Hall, A.R. Katritzky, Synthesis, and QSAR Analysis of Anti-Oncological Active Spiro-alkaloids, Org. Biomol. Chem. 13 (2015) 1741-1753. https://doi.org/10.1039/C4OB02149E

6. A.S. Girgis, S.S. Panda, E.M. Shalaby, A.F. Mabied, P.J. Steel, C.D. Hall, A.R. Katritzky, Regioselective Synthesis and Theoretical Studies of an Anti-neoplastic Fluoro-substituted Dispiro-oxindole, RSC Adv. 5 (2015) 14780-14788. https://doi.org/10.1039/C4RA13433H

7. A.S. Girgis, S.S. Panda, M.N. Aziz, P.J. Steel, C.D. Hall, A.R. Katritzky, Rational Design, Synthesis, and 2D-QSAR Study of Anti-Oncological Alkaloids Against Hepatoma and Cervical Carcinoma, RSC Adv. 5 (2015) 28554-28570. https://doi.org/10.1039/C4RA16663A

8. Y. Kia, H. Osman, R.S. Kumar, V. Murugaiyah, A. Basiri, S. Perumal, I.A. Razak, A Facile Chemo-, Regio- and Stereoselective Synthesis and Cholinesterase Inhibitory Activity of Spirooxindole-Pyrrolizine-Piperidine Hybrids, Bioorg. Med. Chem. Lett. 23 (2013) 2979–2983. https://doi.org/10.1016/j.bmcl.2013.03.027

9. A.I. Almansour, R.S. Kumar, N. Arumugam, A. Basiri, Y. Kia, M.A. Ali, M. Farooq, V. Murugaiyah, A Facile Ionic Liquid Promoted Synthesis, Cholinesterase Inhibitory Activity and Molecular Modelling Study of Novel Highly Functionalized Spiropyrrolidines, Molecules 20 (2015), 2296–2309. https://doi.org/10.3390/molecules20022296

10. A. Basiri, B.M. Abd Razik, M.O. Ezzat, Y. Kia, R.S. Kumar, A.I. Almansour, N. Arumugam, V. Murugaiyah, Synthesis and Cholinesterase Inhibitory Activity Study of

New Piperidone Grafted Spiropyrrolidines, Bioorg. Chem. 75 (2017) 210–216. https://doi.org/10.1016/j.bioorg.2017.09.019

11. A. Toumi, S. Boidriga, K. Hamden, M. Sobeh, M. Cheurfa, M. Askri, M. Knorr, C. Strohmann, L. Brieger, Synthesis, Antidiabetic Activity and Molecular Docking Study of Rhodanine-substituted Spirooxindole Pyrrolidine Derivatives as Novel α-amylase Inhibitors, Bioorg. Chem. 106 (2021) 104507-104524. https://doi.org/10.1016/j.bioorg.2020.104507

12. S. Haddad, S. Boudriga, T.N. Akhaja, J.P. Raval, F. Porzio, A. Soldera, M. Askri, M. Knorr, M.K. Marek, D.A. Rajani, A Strategic Approach to the Synthesis of Functionalized Spirooxindole Pyrrolidine Derivatives: *In Vitro* Antibacterial, Antifungal, Antimalarial and Antitubercular Studies, New J. Chem. 39 (2015) 520–528. https://doi.org/10.1039/C4NJ01008F

13. A. Dandia, S. Khan, P. Soni, A. Indora, D.K. Mahawar, P. Pandya, C.S. Chauhan, Diversity-oriented Sustainable Synthesis of Antimicrobial Spiropyrrolidine/ Thiapyrrolizidine Oxindole Derivatives: New Ligands for a *Metallo-β-lactamase* from *Klebsiella pneumonia*, Bioorg. Med. Chem. Lett. 27 (2017) 2873–2880. https://doi.org/10.1016/j.bmcl.2017.04.083

14. Y.X. Song, D.M. Du, Asymmetric Construction of Bispiro[oxindole-pyrrolidinerhodanine]s via Squaramide-catalyzed Domino Michael/Mannich [3+2] Cycloaddition of Rhodanine Derivatives with *N*-(2,2,2-Trifluoroethyl)isatin Ketimines, J. Org. Chem. 83 (2018) 9278–9290. https://doi.org/10.1021/acs.joc.8b01245

15. S.M. Rajesh, S. Perual, J.C. Menéndez, P. Yogeeswai, D. Sriram, Antimycobacterial Activity of Spirooxindolo-pyrrolidine, Pyrrolizine and Pyrrolothiazole Hybrids Obtained

by a Three-component Regio- and Stereoselective 1,3-Dipolar Cycloaddition, Med. Chem. Commun. 2 (2011) 626-630. https://doi.org/10.1039/C0MD00239A

16. K. Lundahl, J. Schut, J.L.M.A. Schlatmann, G.B. Paerels, A. Peters, Synthesis and Antiviral Activities of Adamantane Spiro Compounds. 1. Adamantane and Analogous Spiro-3′-Pyrrolidines, J. Med. Chem. 15 (1975) 129-133. https://doi.org/10.1021/jm00272a003

17. M.J. Kornet, A.P. Thio, Oxindole-3-spiropyrrolidines and -piperidines. Synthesis and Local Anesthetic Activity, J. Med. Chem. 19 (1976) 892-898. https://doi.org/10.1021/jm00229a007

18. M.A. Abou-Gharbia, P.H. Dokas, Synthesis of Tricyclic Arylspiro Compounds as Potential Antileukemic and Anticonvulsant Agents, Heterocycles 12 (1979) 637-640. https://doi.org/10.3987/R-1979-05-0637

19. World Health Organization (WHO) – Dementia (2020, September 21). [Online]. Available from https://www.who.int/news-room/fact-sheets/detail/dementia. (Accessed on 23 February 2022]

20. K. Ito, S. Ahadieh, B. Corrigan, J. French, T. Fullerton, T. Tensfeldt, Disease Progression *Meta*-analysis Model in Alzheimer's Disease, Alzheimers & Dement. 6 (2010) 39–53. https://doi.org/10.1016/j.jalz.2009.05.665

21. P.J. Houghton, M.-J. Howes, Natural Products and Derivatives Affecting Neurotransmission Relevant to Alzheimer's and Parkinson's Disease, Neurosignals 14 (2005) 6–22. https://doi.org/10.1159/000085382

22. V. Revadigar, R.M. Chalib, V. Murugaiyah, M.A. Embaby, A. Jawad, S.H. Mehdi, R. Hashim, O. Sulaiman, Enzyme Inhibitors Involved in the Treatment of Alzheimers Disease.

In: Frontier in Drug Design and Discovery, Bentham Science Publishers 6 (2014) 142-198. https://doi.org/10.1016/B978-0-12-803959-5.50003-9

23. M. Krátký, S. Štepánková, N-H. Houngbedji, R. Vosátka, K. Vorcáková, J. Vinšová, 2-Hydroxy-*N*-phenylbenzamides and Their Esters Inhibit Acetylcholinesterase and Butyrylcholinesterase, Biomolecules 9 (2019) 698-714. https://doi.org/10.3390/biom9110698

24. M.A. Ali, V.S. Lakshmipathi, F. Beevi, R.S. Kumar, R. Ismail, T.S. Choon, A.C. Wei, Y.K. Yoon, A. Basiri, Antimycobacterial Activity: Synthesis and Biological Evaluation of Novel Subtituted (3*E*,5*E*)-3,5-Diarylidene-1-phenethylpiperidine-4-one Derivatives, Lett. Drug Des. Discov. 10 (2013) 471-476. https://doi.org/10.2174/1570180811310050015

25. M. A. Ali, J. G. Sami, E. Manogaran, V. Sellapan, M. Z. Hassan, M. J. Ahsan, S. Pandian, M. ShaharYar, Synthesis and Antimycobacterial Evaluation of Novel 5,6-Dimethoxy-1-oxo-2,5-dihydro-1H-2-indenyl-5,4-substituted Phenyl Methanone Analogues, Bioorg. Med. Chem. Lett. 19 (2009) 7000−7002. https://doi.org/10.1016/j.bmcl.2009.10.034

26. G.L. Ellman, K.D. Courtney, V. Andres, R.M. Featherstone, A New and Rapid Colorimetric Determination of Acetylcholinesterase Activity, Biochem. Pharmacol. 7 (1961) 88–95. https://doi.org/10.1016/0006-2952(61)90145-9

27. K.Y. Khaw, S.B. Choi, S.C. Tan, H.A. Wahab, K.L. Chan, V. Murugaiyah, Prenylated Xanthones from Mangosteen as Promising Cholinesterase Inhibitors and Their Molecular Docking Studies, Phytomed. 21 (2014) 1303–1309. https://doi.org/10.1016/j.phymed.2014.06.017

28. E.F. Pettersen, T.D. Goddard, C.C. Huang, G.S. Couch, D.M. Greenblatt, E.C. Meng, T.E. Ferrin, UCSF Chimera–A Visualization System for Exploratory Research and Analysis, J. Comput. Chem. 25 (2004) 1605-1612. https://doi.org/10.1002/jcc.20084

29. J. Wang, W. Wang, P.A. Kollman, D.A. Case, Automatic Atom Type and Bond Type Perception in Molecular Mechanical Calculation, J. Mol. Graph. Model. 25 (2006) 247-260. https://doi.org/10.1016/j.jmgm.2005.12.005

30. C.C. Huang, E.C. Meng, J.H. Morris, E.F. Pettersen, T.E. Ferrin, Enhancing UCSF Chimera Through Web Services, Nucleic Acid Res. 42 (2014) 478-484. https://doi.org/10.1093/nar/gku377

31. A.A. Raj, R. Raghunathan, A High Regioselective Synthesis of Novel Dispiro[oxindole-cyclohexanone]pyrrolidines, Syn. Commun. 33 (2003) 421-426. https://doi.org/10.1081/SCC-120015772

32. X. Li, X. Yu, P. Yi, Synthesis of Novel Trispiroheterocycles Through 1,3-Dipolar Cycloaddition of Azomethine Ylides and Nitrile Oxide, Chinese J. Chem. 28 (2010) 434-438. https://doi.org/10.1002/cjoc.201090092

33. E.M. Shalaby, A.S. Girgis, A.M. Moustafa, A.M. Elshaabiny, B.E.M. El-Gendy, A.F. Mabied, F. Ahmed, Regioselective Synthesis, Stereochemical Structure, Spectroscopic Characterization and Geometry Optimization of Dispiro[3*H*-indole-3,2′-pyrrolidine-3′,3″-piperidines], J. Mol. Struct. 1075 (2014) 327-334. https://doi.org/10.1016/j.molstruc.2014.07.014

34. A.C. Wei, M.A. Ali, Y.K. Yoon, R. Ismail, T.S. Choon, K.Y. Khaw, V. Murugaiyah, V.S. Lakshmipathi, Synthesis of Highly Functionalised Dispiropyrrolidine Derivatives as Novel Acetycholinesterase Inhibitors, Lett. Drug Des. Discov. 11 (2014) 156-161. https://doi.org/10.2174/15701808113109990038

35. R.S. Kumar, S. Perumal, Novel Three-Component Tandem Reactions of Cyclic Mono Ketones, Isatin and Sarcosine: Formation of Dispiropyrrolidines, Tetrahedron Lett. 48 (2007) 7164-7168. https://doi.org/10.1016/j.tetlet.2007.07.197

36. H.M.E. Hassaneen, E.M. Eid, H.A. Eid, T.A. Farghaly, Y.N. Mabkhot, Facial Regioselective Synthesis of Novel Bioactive Spiropyrrolidine/Pyrrolizine-Oxindole Derivatives via a Three Components Reaction as Potential Antimicrobial Agents, Molecules 22 (2017) 1–15. https://doi.org/10.3390/molecules22030357

37. R.M. Lane, S.G. Potkin, A. Enz, Targeting Acetylcholinesterase and Butyrylcholinesterase in Dememtia, Int. J. Neuropharmacol. 9 (2006) 101-124. https://doi.org/10.1017/S1461145705005833

38. C. Roca, C. Requena, V. Sebastián-Pérez, S. Malhotra, C. Radoux, C., Pérez, A. Martinez, J.A. Páez, T.L. Blundell, N.E. Campillo, Identification of New Allosteric Sites and Modulators of AChE Through Computational and Experimental Tools, J. Enzyme Inhib. Med. Chem. 33 (2018) 1034–1047. https://doi.org/10.1080/14756366.2018.1476502

39. C.J. Tsai, A. del Sol, R. Nussinov, Allostery: Absence of A Change in Shape Does Not Imply that Allostery Is Not at Play, J. Mol. Biol. 378 (2008) 1–11. https://doi.org/10.1016/j.jmb.2008.02.034

40. S. Kuruvilla, J. Mukherjee, Suppression of Acetylcholine Breakdown by Butyrylcholinesterase Inhibitor in Postmortem Alzheimer's Disease Brain, J. Nucl. Med. 55 (2014) 416.

41. T.L. Rosenberry, X. Brazzolotto, I.R. Macdonald, M. Wandhammer, M. Trovaslet-Leroy, S. Darvesh, F. Nachon, Comparison of the Binding of Reversible Inhibitors to Human Butyrylcholinesterase and Acetylcholinesterase: A Crystallographic, Kinetic and Calorimetric Study, Molecules 22 (2017) 2098. https://doi.org/10.3390/molecules22122098

42. J. Cheung, E.N. Gary, K. Shiomi, T.L. Rosenberry, Structures of Human Acetylcholinesterase Bound to Dihydrotanshinone I and Territrem B Show Peripheral Site

Flexibility, ACS Med. Chem. Lett. 4 (2013) 1091-1096. https://doi.org/10.1021/ml400304w